Acta Cryst. (1983). B39, 324–329

The Nature of the Chemical Bonding in Boron Carbide. IV. Electronic Band Structure of Boron Carbide, $B_{13}C_2$, and Three Models of the Structure $B_{12}C_3$

BY D. R. ARMSTRONG, J. BOLLAND AND P. G. PERKINS

Department of Pure and Applied Chemistry, University of Strathclyde, Glasgow G1 1XL, Scotland

AND G. WILL AND A. KIRFEL

Mineralogisch-Petrologisches Institut der Universität Bonn, 5300 Bonn, Federal Republic of Germany

(*Received* 28 *September* 1982; *accepted* 26 *January* 1983)

Abstract

A study by band-structure methods of the boron carbide $B_{13}C_2$ is presented. All symmetry directions are considered and it is found that, in general, the valence bands are flat in almost all directions – nowhere does a band width exceed 3 eV (1 eV = $1{\cdot}60 \times 10^{-19}$ J). There is slightly greater curvature in the conduction band. The valence-band structure, containing 47 electrons, is incompletely filled and the Fermi level lies at $-7{\cdot}6$ eV. Above the valence-band edge, a band gap exists amounting to just over 4 eV. The density of states and the partial density of states of the compound are both calculated. Using the density-of-states plots, the bonding in $B_{13}C_2$ is discussed. Total charges on the atoms are calculated from the density of states and the charge-transfer predictions are in satisfactory agreement with those obtained from the crystallographic experiment. The bonding can also be discussed using a cluster approach and, from this, all the bond indices within the unit cell are calculated. Inter-icosahedral bonds are much stronger than are intra-icosahedral bonds, whilst the B—C bonds which lie in the CBC chain show slight multiple-bond character. For the models of $B_{12}C_3$ we find that a $B_{12}C_3$ structure in which a C atom is substituted into an icosahedron is more stable than the one in which the chain bonding consists of C only.

Introduction

At present, there exists some controversy over the precise nature of the compound which is called 'boron carbide'. This compound was initially formulated as B_4C and this formulation was later amended to $B_{12}C_3$. However, more recent definitive work by Kirfel, Gupta & Will (1979*a*,*b*) has cast considerable doubt on any structure with stoichiometry $B_{12}C_3$. Will *et al.* have accumulated considerable evidence which indicates that a stable phase of formula $B_{13}C_2$ exists. This experimental evidence stems essentially from a study of boron–carbon phases (Will & Kossobutzki 1976*a*,*b*). It has been shown that the crystal structure of the $B_{13}C_2$ phase contains icosahedra and CBC chains (Fig. 1) (Kirfel, Gupta & Will, 1979*a*). The B_{12} icosahedra are interconnected by six linear CBC bonds which emanate from each B_{12} unit, whilst each C atom is connected to three B_{12} units. $B_{13}C_2$ is a member of the α-rhombohedral boron series $R\bar{3}m$ and this includes the materials B_{12}, $B_{13}C_2$, $B_{12}P_2$ and $B_{12}As_2$. One finds two types of B atom present in the B_{12} icosahedra: there are atoms which belong to the six-atom equatorial rings around the threefold axis and are usually denoted as B(1) atoms; the second type is found on the two polar triangles with lie on the same threefold axis and these are labelled B(2) atoms. In $B_{13}C_2$ the B(1) atoms are bonded to the CBC chain while the B(2) atoms are responsible for the inter-icosahedral bonding.

In this paper we report the results of calculations on $B_{13}C_2$ and examine the differing bonding roles of the two types of boron, as well as discussing the electronic situation in the linear CBC unit. We also put forward possible structures for $B_{12}C_3$.

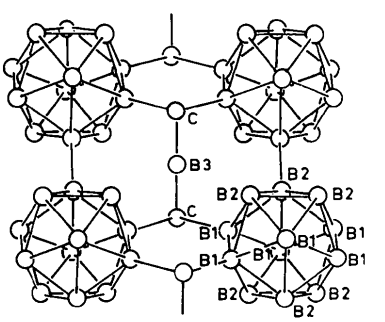

Fig. 1. The structure of $B_{13}C_2$.

0108-7681/83/030324-06$01.50

Calculational method, results, and discussion

The calculational method used has previously been fully described (Armstrong, Breeze & Perkins, 1976, 1977). The Hamiltonian operator is undefined and the basis sets consist of the $2s$, $2p$ valence orbitals of B and C. Orbital overlap was included and hence the eigenvalue problem solved was (H−ES) = 0. The calculations on $B_{13}C_2$ assumed a unit cell of that formula and this was allowed to interact with *ca* 1000 neighbouring unit cells. The input geometrical data and atomic data for the calculation were taken from previous work (Kirfel, Gupta & Will, 1979*a*; Armstrong, Perkins & Stewart, 1971). All symmetry lines of the rhombohedral Brillouin zone (Fig. 2) were studied in the calculation and the band-structure results are shown in Fig. 3. The valence-band structure is rather uninteresting (although significant) in that it exhibits a series of almost flat energy bands, with little variation in energy with symmetry direction. There is a band gap of 4·1 eV and this separates the valence from the conduction bands. The conduction-band structure shows somewhat greater curvature than that of the valence band. The unit cell of $B_{13}C_2$ contains 47 electrons, whilst the valence bands can accommodate 48; hence, the valence bands cannot be completely filled. We consider the consequences of this later in the paper.

The density-of-states function for $B_{13}C_2$ was calculated by a method described previously (Armstrong, Breeze & Perkins, 1977) and is shown in Fig. 4. The Fermi level is calculated to lie at −7·6 eV, whilst the tail of unoccupied valence states extends to −6·7 eV. Next, a convolution of the valence- and conduction-band states is produced by constructing the joint density of states; this function for $B_{13}C_2$ is shown in Fig. 5. The joint-density-of-states function shows that $B_{13}C_2$ should absorb light at all frequencies from zero and should show peaks at *ca* 1 and 3 eV. Of course, in this convolution of states we do not include the transition moments for the excitations; these are all assumed to be unity. Some modification of the absorption picture would, therefore, be found if the transition moments were included but we do not believe that it would be significant.

Table 1 lists the partial density of states near the band edges of the valence and conduction bands. For the valence band, the highest percentage of states near the band edges occurs for the B(2) atoms which are involved in inter-icosahedral bonding and there is also a

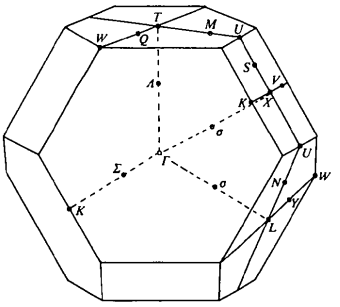

Fig. 2. The Brillouin zone for the rhombohedral Bravais lattice.

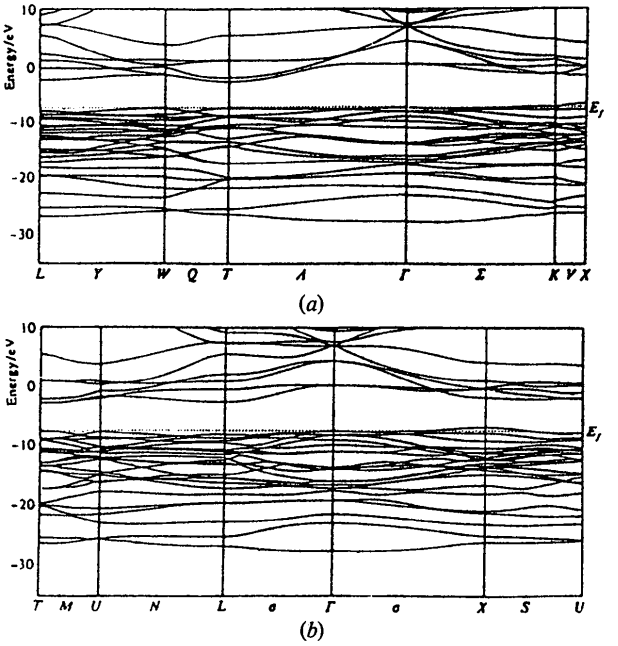

Fig. 3. (*a*), (*b*) Band structure for $B_{13}C_2$.

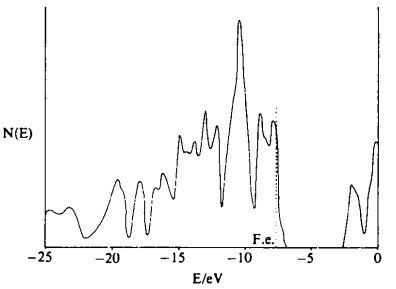

Fig. 4. Total density of states for $B_{13}C_2$.

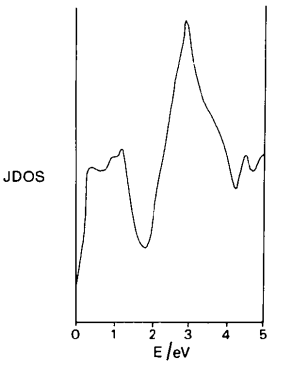

Fig. 5. Joint density of states for $B_{13}C_2$.

Table 1. *Percentage of states at the valence- and conduction-band edges for* $B_{13}C_2$

	B(1)	B(2)	B(3)	C
Valence band (%)	27·5	42·3	7·9	21·2
Conduction band (%)	30·9	20·7	44·3	4·0

significant contribution from the states of the C atoms. For the conduction states, there is a large contribution from the chain boron atom B(3) states – this latter is particularly marked when one recalls that the stoichiometry of the compounds shows a ratio of 6:6:1 in B(1), B(2) and B(3). The partial densities of states for B(1), B(2), B(3) and C are shown in Fig. 6. It is clear that the boron 2*s* states for B(1) and B(2) occur in the lowest-lying energy areas of the band structure, with peaks lying between −18 and −28 eV. The boron 2*p* states occur at much higher energy and produce localized peaks lying near −10eV, the main peak due to B(2) lying lower in energy than that due to the B(1) atoms. It is also noticeable that the density peak from the boron 2*p* orbital of B(2) is larger than that from B(1) at the Fermi level.

The localized nature of the bonding in which B(3) is involved is clearly indicated by the sharp peaks which are extant for the 2*s* and 2*p* orbitals of this atom. The contribution of the B(3) 2*p* orbitals to the conduction band is particularly large in this context. The partial-density-of-states diagram for C exhibits similar features, having two localized 2*s* peaks lying between −22 and −26 eV and six peaks from 2*p* states lying between −6·7 and −20 eV. There is also a large contribution to the Fermi edge states stemming from the carbon 2*p* orbitals.

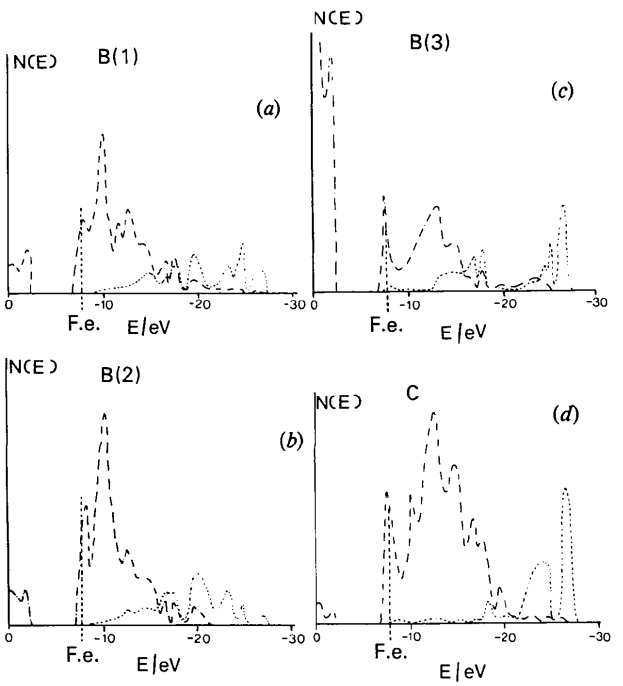

Fig. 6. (*a*)–(*d*) Partial density of states of B(1), B(2), B(3) and C in $B_{13}C_2$ (–·–·– 2*p* contribution, –––– 2*s* contribution).

Electrical properties of $B_{13}C_2$

Since there are only 47 valence electrons in $B_{13}C_2$ and 24 valence bands, then it is clear that there must be some empty states lying at the top of the valence band. This is shown clearly in the total-density-of-states curve (Fig. 4). On the basis of this evidence, one might expect that $B_{13}C_2$ would be a metallic conductor. It has been reported that 'boron carbide' is a semiconductor though this appears to refer to material of a different stoichiometry, *i.e.* $B_{12}C_3$ (Werheit, 1979; Werheit, Binnenbruck & Hansen, 1971).

Werheit has recently investigated the electrical conductivity of samples of 'boron carbide' with varying carbon composition (Werheit, De Groot & Malkemper, 1981). He reports the conductivity at the composition corresponding to $B_{13}C_2$ as 10 Ω^{-1} cm^{-1} at 300 K, and ascribes the conductivity to variable-range hopping. Increase of the carbon content of the samples lowers the conductivity and a minimum appears at the composition $B_{12}C_3$. Thereafter the conductivity increases with added carbon content. In the latter regime the conductivity is supposed to stem from metal-like impurity-band conductivity.

It is fairly clear that, although $B_{13}C_2$ would appear to be a metallic conductor from our calculations, the conductivity will, in any case, be somewhat limited. The specific electrical conductivity of a material is given by $\sigma = ne\mu$, where n is the number of charge carriers, and μ is their mobility. The number of charge carriers at the Fermi edge will depend on the number of occupied levels in that region (or for holes of the unoccupied levels). It can be seen that for $B_{13}C_2$ this is not particularly large ($11{\cdot}0 \times 10^{40}$ J^{-1} cm^{-3}). Hence, σ will be limited by this factor. In addition, the mobility of an electron in a solid is governed by properties which include both its tendency to suffer attenuation from various modes of scattering and the effective mass of the electron/hole in the bands which afford the conductivity. The square of the effective mass of an electron is inversely proportional to its mobility and the effective mass is, essentially, dominated by the curvature of the bands. Since the bands in the ultimate unoccupied valence region of $B_{13}C_2$ have little curvature, it is clear that the effective mass of the electron will be high. The equation for extended band conductivity in such a solid is given by

$$\sigma = 2\pi^2 e^2 \hbar^3 a \frac{1}{m^{*2}} [N(E_f)]^2$$

and, hence, taking the effective mass, m^*, to be 10 (which corresponds to flat bands), we find an electrical conductivity $\sigma \simeq 526\ \Omega^{-1}\ cm^{-1}$. This is low, in keeping with experimental evidence.

We can now advance a simple interpretation of Werheit's experimental results (Werheit, De Groot & Malkemper, 1981). Increase of the carbon content of the 'boron carbide' will provide extra electrons which, consequently, will decrease the number of vacant states at the Fermi edge in the valence band. Hence, the metallic conductivity would decrease on going from $B_{13}C_2$ to $B_{12}C_3$. In the latter compound, there are exactly 48 electrons in 24 orbitals and the material is a semiconductor with a band gap lying between 2·9–4·0 eV. Further increase in the carbon content would cause occupation of the conduction bands, with the re-establishment of metallic conductivity.

Cluster calculations

In addition to the band-structure calculations for $B_{13}C_2$, we carried out a series of cluster calculations. This type of calculation has been fully described previously (Perkins & Stewart, 1980). In essence, a cluster calculation is a pseudomolecular calculation using a representative part of the crystal structure with superimposition of the Born–von Karman boundary conditions. The calculation is computationally simpler than the full band-structure approach and hence it is possible to make the results self-consistent with respect to charge distribution. This yields a better view of the latter than does the band structure. All the crystal interactions are included and the principal advantage of such a calculation is that one can obtain a view of the bonding in the crystal which is not readily obtainable from the full band-structure approach. We can calculate the electron-population distribution through all the constituent atomic orbitals, as well as the bond indices (Armstrong, Perkins & Stewart, 1973*a*,*b*) for all constituent bonds. This enables us to make comparisons between bonds in terms of their intrinsic strength. The cluster electron distribution and the bond indices are listed in Table 2.

We note, first of all, that all the intra-icosahedral bonds exhibit an index amounting to *ca* 0·50. This is substantially the same as one finds from a calculation on the isolated $B_{12}H_{12}^{2-}$ ion (Armstrong, Perkins & Stewart, 1973*c*). Since bond-index values can be directly and linearly correlated with bond strength (Bell & Perkins, 1975, 1977), then it is clear that the B–B intra-icosahedral bond is about half as strong as a normal B–B bond. From previous calculations (Laurie & Perkins, 1982) of the intrinsic B–B bond energy, we therefore find an intrinsic bond energy for the icosahedron of 149 kJ mol^{-1}. If the bond indices emanating from a single B atom are added up, then one finds the valency of the B atom (Armstrong, Perkins & Stewart, 1973*a*) and, in the case of the icosahedral B atoms, this valency averages 3·69. It is interesting to note that the inter-icosahedral bonds are of considerably greater strength – indeed, the B–B inter-icosahedral bond index is larger than that of the B–C linkage. The former amounts to 0·96 and, hence, from previous reasoning, its intrinsic bond strength amounts to 286 kJ mol^{-1}. The B–C bonds within the CBC chain fragment show a tendency to multiple bonding and may aid in the transfer of electrons along this chain. The multiple-bond-index character of each atom in the structure explains well its general stability. Each atom is bonded into the lattice by ~1050 kJ (g atom)$^{-1}$ and this figure approaches that of diamond [~1340 kJ (g atom)$^{-1}$].

As stated above, the sum of the bond indices about each atom is equal to the valency of the atom and these are also given in Table 2. For B(1), B(2) and C, the valencies are close to the maximum of 4 which can be exhibited by these atoms. The B in the chain, B(3), exhibits a relatively low valency and the 'unbondedness' of this atom leads, hence, to its constituting a reactive centre.

Table 2. *Bond indices and valencies of* $B_{13}C_2$ *obtained from a cluster calculation*

Bond indices		Valencies	
B(1)–B(1)	0·50	B(1)	3·64
B(1)–B(2)	0·49	B(2)	3·75
B(2)–B(2)	0·52	B(3)	3·24
B(2)–B(2′)	0·96	C	3·89
B(3)–C	1·05		
B(1)–C	0·83		

Electron density distribution

The electron density distribution is given for both the band-structure calculation (in which it is calculated from the partial density of occupied states) and the cluster calculation. Table 3 shows the results obtained.

Table 3. *The electron distribution in* $B_{13}C_2$ *obtained from a density-of-states calculation and a cluster calculation*

	Electron populations			Charge	Charge on B_{12} unit	Charge on CBC chain
	s	*p*	Total			
Density-of-states calculation						
B(1)	0·79	2·01	2·80	0·20 e		
B(2)	0·87	2·29	3·16	−0·16	+0·33 e	−0·33 e
B(3)	0·80	1·39	2·19	+0·81		
C	1·15	3·42	4·57	−0·57		
Cluster calculation						
B(1)	0·63	2·21	2·84	+0·16		
B(2)	0·69	2·46	3·15	−0·15	+0·08	−0·08
B(3)	0·74	1·64	2·38	+0·62		
C	0·89	3·46	4·35	−0·35		

Table 4. *The band gap and electron distribution in the* $B_{12}C_3$ *models*

	Valence band edge (eV)	Conduction band edge (eV)	Band gap (eV)	Charge (e) on B(1)	Charge (e) on B(2)	Charge (e) on icosahedra
$B_{12}C_3$ (i)	−6·8	−2·8	4·0	+0·12, +0·22	−0·22, −0·11	+0·16
$B_{12}C_3$ (ii)	−6·7	−3·0	3·7	+0·22, +0·11	−0·12, −0·22	+0·30
$B_{12}C_3$ (iii)	−7·1	−4·2	2·9	+0·16	−0·21	−0·33

From the band-structure calculation, it can be seen that there is, overall, a charge migration from the B_{12} icosahedron to the CBC chain. This charge originates mainly from the B(1) equatorial atoms but there is also a drift from the B(1) to the B(2) atoms within the B_{12} icosahedron. The electron-density distribution within the CBC chain itself shows that there is an electron drift from the B(3) atom to each C atom. These electron shifts are in agreement with the expected values based essentially on the differing electronegativities of B and C.

Electron densities obtained from the cluster calculations show qualitative agreement with those based on the density-of-states calculation. Those stemming from the latter are probably more reliable, since they are self-consistent. The electron transfer in the latter is much smaller and the CBC linkage receives only 0·10 electrons from the B_{12} icosahedron. These charge shifts are in qualitiative agreement with those which have been calculated from the crystal structure data (Kirfel, Gupta & Will, 1979*a*).

$B_{12}C_3$

In this case, we constructed a structure corresponding to the stoichiometry $B_{12}C_3$ by supposing that this structure is a C-substituted derivative of $B_{13}C_2$. This involves substituting a B by a C atom. Such a substitution could create three possible structures: (i) $B_{11}C$–CBC, where a B(1) atom is substituted; (ii) $B_{11}C$–CBC, where a B(2) atom is substituted; and (iii) B_{12}–CCC, where the B(3) atom is substituted. The total energy per unit cell for each of these three structures was calculated from the density-of-states calculation and these were, respectively, −710·59, −711·92, and −704·49 eV. We do not regard this energy calculation as reliable enough to differentiate between structures of types (i) and (ii) but it is fairly clear that these two structures are considerably more stable than that of type (iii). We can, hence, conclude that, in the $B_{12}C_3$ phase, C is not likely to appear in the inter-icosahedral chains.

NMR studies of Silver & Bray (1959), and IR studies of Becher & Thevenot (1974) also lead to the conclusion that the central position in the linear triatomic group is occupied by a B rather than a C atom. Recent work by Bouchacourt & Thevenot (1981) on the lattice parameters of the boron–carbon compounds suggests that the C substitution in $B_{12}C_3$ seems to occur on the rhombohedral B(2) sites in line with our total energy per unit cell calculations. The greater stability of the $B_{12}C_3$ type (ii) compound is connected with the greater number of B–C bonds formed by substitution.

The band gap and electron distribution for the stable structures are shown in Table 4. In all cases, the gap between the valence- and conduction-band manifolds is lower than that recorded for $B_{13}C_2$. However, it is interesting that the band gap here represents the absorption edge and, hence, we would expect a material with the formula $B_{12}C_3$ to be, firstly, an insulator or semiconductor and, secondly, to show absorption at all energy frequencies starting above that of the band gap. Exciton effects would modify the absorption edge, however.

The charge differential between B(1) and B(2) atoms found in $B_{13}C_2$ is also maintained in the $B_{12}C_3$ series. The substitution of B by C in the icosahedron increases the electron drift to the linear chain while substitution in the linear chain brings about electron donation to the B_{12} unit. In each type of $B_{12}C_3$ molecule, the substituted C atom carries a positive charge.

One of us (JB) thanks the SERC for a Maintenance Grant.

References

ARMSTRONG, D. R., BREEZE, A. & PERKINS, P. G. (1976). *J. Phys. C*, **8**, 3558–3570.

ARMSTRONG, D. R., BREEZE, A. & PERKINS, P. G. (1977). *J. Chem. Soc. Faraday Trans.* 2, **73**, 952–957.

ARMSTRONG, D. R., PERKINS, P. G. & STEWART, J. J. P. (1971). *J. Chem. Soc. A*, pp. 3674–3679.

ARMSTRONG, D. R., PERKINS, P. G. & STEWART, J. J. P. (1973*a*). *J. Chem. Soc. Dalton Trans.* pp. 838–840.

ARMSTRONG, D. R., PERKINS, P. G. & STEWART, J. J. P. (1973*b*). *J. Chem. Soc. Dalton Trans.* pp. 2273–2277.

ARMSTRONG, D. R., PERKINS, P. G. & STEWART, J. J. P. (1973*c*). *J. Chem. Soc. Dalton Trans.* pp. 627–632.

BECHER, H. J. & THEVENOT, F. (1974). *Z. Anorg. Allg. Chem.* **410**, 274–286.

BELL, T. N. & PERKINS, P. G. (1975). *Nature (London)*, **256**, 300–301.

BELL, T. N. & PERKINS, P. G. (1977). *J. Phys. Chem.* **81**, 2012–2016.

BOUCHACOURT, M. & THEVENOT, F. (1981). *J. Less-Common Met.* **82**, 227–235.

KIRFEL, A., GUPTA, A. & WILL, G. (1979*a*). *Acta Cryst.* B**35**, 1052–1059.

KIRFEL, A., GUPTA, A. & WILL, G. (1979*b*). *Acta Cryst* B**35**, 2291–2300.
LAURIE, D. & PERKINS, P. G. (1982). *Inorg. Chim. Acta.* In the press.
PERKINS, P. G. & STEWART, J. J. P. (1980). *J. Chem. Soc. Faraday Trans.* 2, **76**, 520–533.
SILVER, A. H. & BRAY, P. J. (1959). *J. Chem. Phys.* **31**, 247–253.
WERHEIT, H. (1979). *J. Less-Common Met.* **67**, 143–148.
WERHEIT, H., BINNENBRUCK, H. & HANSEN, A. (1971). *Phys. Status Solidi B*, **47**, 153–159.
WERHEIT, H., DE GROOT, K. & MALKEMPER, W. (1981). *J. Less-Common Met.* **82**, 153–162.
WILL, G. & KOSSOBUTZKI, K. H. (1976*a*). *J. Less-Common Met.* **44**, 87–97.
WILL, G. & KOSSOBUTZKI, K. H. (1976*b*). *J. Less-Common Met.* **47**, 43–48.

Acta Cryst. (1983). B**39**, 329–336

Structures of Complexes between Dimethylthallium Picrate and Two Isomers of Dicyclohexano-18-crown-6*

BY DAVID L. HUGHES AND MARY R. TRUTER†

Molecular Structures Department, Rothamsted Experimental Station, Harpenden, Hertfordshire AL5 2JQ, England

(*Received* 12 *October* 1982; *accepted* 23 *November* 1982)

Abstract

The crystal structures of complexes formed by dimethylthallium picrate with two isomers of dicyclohexano-18-crown-6 have shown that in both there are $[Me_2Tl\ crown]^+$ cations and picrate anions, the complex cations consisting of linear Me_2Tl entities normal to the plane through the six O atoms of the ligand and the Tl atom. For isomer *A*, *cis-cisoid-cis*-dicyclohexano-18-crown-6, the complex **A** is formed: $[Tl(CH_3)_2(C_{20}H_{36}O_6)].C_6H_2N_3O_7$, $C_{22}H_{42}O_6Tl^+.C_6H_2N_3O_7^-$, M_r = 835·0, triclinic, $I\bar{1}$ (variation of $P\bar{1}$), a = 11·359 (2), b = 19·772 (3), c = 14·904 (2) Å, α = 95·55 (1), β = 90·65 (1), γ = 94·58 (1)°, V = 3320·5 Å^3, Z = 4, D_x = 1·670 g cm^{-3}, Mo $K\alpha$, λ = 0·71069 Å, μ = 49·8 cm^{-1}, $F(000)$ = 1672, R = 0·036 for 3067 reflections with above zero intensities. The cation has an approximate plane of symmetry through the dimethylthallium group and the O atoms in $-CH_2-O-CH_2-$ groups. This gives a different conformation for the ligand from that, with approximate 2 symmetry, in other complexes of isomer *A*. For isomer *B*, *cis-transoid-cis*-dicyclohexano-18-crown-6, the complex **B** is formed: $[Tl(CH_3)_2(C_{20}H_{36}O_6)].C_6H_2N_3O_7$, $C_{22}H_{42}O_6Tl^+.C_6H_2N_3O_7^-$, M_r = 835·0, triclinic, $P\bar{1}$, a = 8·137 (2), b = 8·205 (3), c = 13·201 (3) Å, α = 94·16 (2), β = 96·71 (2), γ = 108·63 (3)°, V = 823·8 Å^3, Z = 1, D_x = 1·683 g cm^{-3}, Mo $K\alpha$, λ = 0·71069 Å, μ = 50·1 cm^{-1}, $F(000)$ = 418, R = 0·038 for all 2142 (all observed) reflections. The Tl atom lies on, and the picrate anion is disordered about, centres of symmetry. The conformation of the ligand with $\bar{1}$ symmetry is the same as that found in the sodium complex. In both complexes, on each cyclohexane ring one O atom is axially and one equatorially substituted; these are at significantly different distances from the Tl atom, the former giving the longer bond. An explanation, applicable also to other complexes, is that of steric hindrance between the equatorial H atom on a cyclohexane carbon and a H atom of the macrocyclic ring.

Introduction

Comparison of the formation constants for dibenzo-18-crown-6 and the two isomers obtained by hydrogenation with *cis* substitution on the ring junctions shows that the *cis-cisoid-cis* isomer *A* has a higher value than the *cis-transoid-cis* isomer *B*. (Formulae are in Fig. 1.) According to the cation and solvent, however, the value of the formation constant for dibenzo-18-crown-6 may be higher or lower than or between isomers *A* and *B* (Frensdorff, 1971; Izatt *et al.*, 1976). This is unexpected because O atoms attached to aliphatic C atoms are normally more electronegative than those attached to aromatic C atoms, consistent with the value for dibenzo-18-crown-6 being the lowest. Similar variations in formation constant are found for macrobicyclic compounds, the [222], [benzo 222] and [dibenzo 222] cryptands (Lehn, 1973) and Parsons'

* Complex **A**: (*cis-cisoid-cis*-5,8,11,16,19,22-hexaoxaperhydrodibenzo[*a*,*j*]cyclooctadecene)dimethylthallium(III) picrate; complex **B**: (*cis-transoid-cis*-5,8,11,16,19,22-hexaoxaperhydrodibenzo[*a*,*j*]cyclooctadecene)dimethylthallium(III) picrate.

† To whom all correspondence should be addressed.

0108-7681/83/030329-08$01.50